

## Half-metallic properties of atomic chains of carbon–transition-metal compounds

S. Dag,<sup>1</sup> S. Tongay,<sup>1</sup> T. Yildirim,<sup>2</sup> E. Durgun,<sup>1</sup> R. T. Senger,<sup>1</sup> C. Y. Fong,<sup>3</sup> and S. Ciraci<sup>1,\*</sup>

<sup>1</sup>*Department of Physics, Bilkent University, Ankara 06800, Turkey*

<sup>2</sup>*NIST Center for Neutron Research, National Institute of Standards and Technology, Gaithersburg, Maryland 20899, USA*

<sup>3</sup>*Department of Physics, University of California, Davis, California 95616, USA*

(Received 19 May 2005; published 31 October 2005)

We found that magnetic ground state of one-dimensional atomic chains of carbon–transition-metal compounds exhibit half-metallic properties. They are semiconductors for one spin direction, but show metallic properties for the opposite direction. The spins are fully polarized at the Fermi level and net magnetic moment per unit cell is an integer multiple of Bohr magneton. The spin-dependent electronic structure can be engineered by changing the number of carbon atoms and type of transition metal atoms. These chains, which are stable even at high temperatures and some of which keep their spin-dependent electronic properties even under moderate axial strain, hold the promise of potential applications in nanospintronics.

DOI: [10.1103/PhysRevB.72.155444](https://doi.org/10.1103/PhysRevB.72.155444)

PACS number(s): 61.46.+w, 71.20.Be, 72.25.–b, 75.50.Cc

### I. INTRODUCTION

Spin-dependent electronic transport has promised revolutionary applications using giant magnetoresistance in magnetic recordings and nonvolatile memories.<sup>1–3</sup> Half metals (HM)<sup>4,5</sup> are a class of materials, which exhibits spin-dependent electronic properties relevant to spintronics. In HMs, due to broken spin degeneracy, energy bands  $E_n(\mathbf{k}, \uparrow)$  and  $E_n(\mathbf{k}, \downarrow)$  split and each band accommodates one electron per  $\mathbf{k}$  point. Furthermore, they are semiconductors for one spin direction, but show metallic properties for the opposite spin direction. Accordingly, the difference between the number of electrons of different spin orientations in the unit cell,  $N=N_{\uparrow}-N_{\downarrow}$ , must be an integer and hence the spin polarization at the Fermi level,  $P=[D(E_F, \uparrow)-D(E_F, \downarrow)]/[D(E_F, \uparrow)+D(E_F, \downarrow)]$ , is complete.<sup>5</sup> This situation is in contrast with the ferromagnetic metals, where both spin directions contribute to the density of states at  $E_F$  and spin polarization  $P$  becomes less than 100%. Even though three-dimensional (3D) ferromagnetic Heusler alloys and transition-metal oxides exhibit half-metallic properties,<sup>6</sup> they are not yet appropriate for spintronics because of difficulties in controlling stoichiometry and the defect levels destroying the coherent spin transport. Zinc-blende (ZB) HMs with high magnetic moment  $\mu$  and high Curie temperature  $T_c > 400$  K (such as CrAs and CrSb in ZB structure) have been grown only in thin-film forms.<sup>7</sup> More recently, it has been predicted that four new ZB crystals can be HM at or near their respective equilibrium lattice constants.<sup>8,9</sup>

In this paper, we report that very simple and stable one-dimensional (1D) structures, such as linear atomic chains of carbon–transition-metal compounds, i.e.,  $C_n(\text{TM})$ , show half-metallic properties. The prediction of half-metallic behavior in 1D atomic chains is new and of fundamental interest, in particular in the field of fermionic excitations with spin degree of freedom. Besides, the present finding may lead to potential applications in the rapidly developing field of nanospintronics, such as tunneling magnetoresistance, spin valve, and nonvolatile magnetic devices.

In earlier transport studies, the spin direction of conduction electrons was generally disregarded, in spite of the fact

that the spin orientation of electrons decays much slower than their momentum.<sup>3</sup> The magnetic ground state of transition metal (TM) adsorbed single-wall carbon nanotubes (SWNTs),<sup>10–12</sup> spontaneous spin-polarized electron transport through finite TM wires,<sup>13</sup> and oscillatory spin-polarized conductance and spin-valve effects through finite carbon wires capped with Co atoms in between gold electrodes<sup>14</sup> have been treated recently. However, half metallicity predicted in periodic  $C_n(\text{TM})$  is a behavior fundamentally different from those magnetic properties found in earlier systems in Refs. 10–14 and is a unique feature of 1D systems that allows both semiconducting and metallic properties coexisting in the same structure.

### II. METHOD

Our predictions are obtained from the first-principles pseudopotential plane wave calculations within density functional theory<sup>15</sup> (DFT) using generalized gradient approximation (GGA)<sup>16</sup> and ultrasoft pseudopotentials.<sup>17</sup>  $C_n(\text{TM})$  chains have been treated in supercell geometry using supercell lattice parameter  $a=10$  Å,  $b=10$  Å, and  $c=c_{lc}$  [ $c_{lc}$  being the axial lattice parameter of the  $C_n(\text{TM})$  linear chain]. In order to investigate Peierls instability, supercells of  $c=2c_{lc}$  comprising two units of  $C_n(\text{TM})$  have been used. The Brillouin zone has been sampled by 10–80 special  $\mathbf{k}$  points depending on the supercell size.<sup>18</sup> Bloch wave functions have been expanded by plane waves having kinetic energy  $\hbar^2|\mathbf{k} + \mathbf{G}|^2/2m \leq 350$  eV. All the atomic positions and the supercell lattice parameter  $c$  along the chain axis are optimized by minimizing the total energy,  $E_T^{sp}$ , the forces on the atoms, as well as the stress of the system calculated by spin-polarized (or spin-relaxed) GGA. Since  $\Delta E = E_T^{su} - E_T^{sp}$  (where  $E_T^{su}$  is spin-unpolarized total energy) and net magnetic moment  $\mu$  are both positive, these compound chains have ferromagnetic ground state.<sup>19</sup> While our study has covered a large family of  $C_n(\text{TM})$  compound chains (TM=Cr, Ti, Mn, Fe), our discussion will focus on  $C_n\text{Cr}$ .

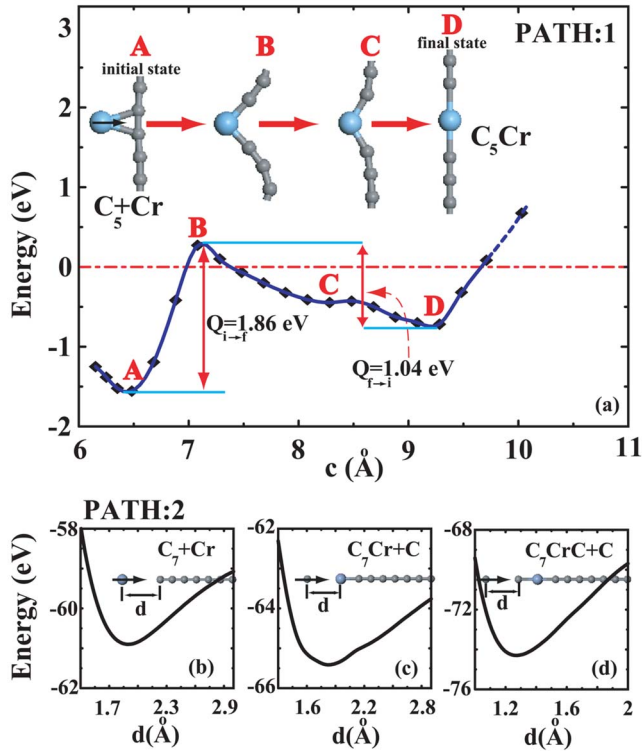


FIG. 1. (Color online) Transition state analysis for two different reaction paths. (a) Path 1: Variation of energy,  $E_T(c)$ , for the transition from the  $C_5+Cr$  initial state to the linear  $C_5Cr$  HM as final state:  $Q_{i \rightarrow f}$  and  $Q_{f \rightarrow i}$  are energy barriers involved in the transitions. Zero of energy is taken relative to the free Cr atom and free periodic C linear chain. (b)–(d) Path 2: Variation of interaction energy with distance  $d$  between  $C_7$  and Cr,  $C_7Cr$  and C,  $C_7CrC$  and C for adatom attaching from one end.

### III. STABILITY OF LINEAR CHAIN STRUCTURES

The finite-size linear chains of carbon atoms have already been synthesized experimentally.<sup>20</sup> The double bond between carbon atoms and doubly degenerate  $\pi$  band crossing the Fermi level underlie the stability of the chain and its unusual electronic properties.<sup>21</sup> We examine the formation of linear  $C_5Cr$  HM by performing transition state analysis along two different reaction paths. Normally, a Cr atom is attracted by a C linear chain and eventually forms a bridge bond over a C—C bond. We take this bound state (specified as  $C_5+Cr$  as an initial state of the first reaction path for the transition to the final state corresponding to the linear  $C_5Cr$  HM as illustrated in Fig. 1(a).<sup>22</sup> The energy barrier necessary to go from the initial state to the final state is  $Q_{i \rightarrow f} = 1.86$  eV. Once the final state has formed, it is prevented from going back to the initial state by a significant barrier of  $Q_{f \rightarrow i} = 1.04$  eV. However, the energy barrier  $Q_{i \rightarrow f}$  disappears totally and hence the process becomes exothermic for the second reaction path where HM is grown from one end of the chain by attaching first the Cr atom then the C atoms sequentially. Each adatom (Cr or C) is attracted to chain and eventually becomes bound to it as shown in Fig. 1(b)–1(d). This analysis lets us believe that half-metallic  $C_n$ (TM) chains are not only of fundamental interest, but also can be realized experimentally.

TABLE I. Results of spin-polarized first-principle calculations for  $C_nCr$  linear chains.  $\Delta E_T$  is the difference between spin-paired (nonmagnetic) and spin-polarized (magnetic) total energies.  $c_{lc}$  is the optimized 1D lattice parameter.  $\mu$  is the total magnetic moment per unit cell in units of Bohr magneton,  $\mu_B$ . M, S, and HM stand for metal, semiconductor, and half metal, respectively. By convention, majority and minority spins are denoted by  $\uparrow$  and  $\downarrow$ . The numerals in the last column are the band-gap energies in eV.

1D compound	$\Delta E_T$ (eV)	$c_{lc}$ (Å)	$\mu$ ( $\mu_B$ )	Type: $\uparrow$ (eV) $\downarrow$ (eV)
CCr	1.8	3.7	2.0	S: $\uparrow=0.7$ $\downarrow=1.0$
$C_2Cr$	2.8	5.2	4.0	HM: $\uparrow=M$ $\downarrow=3.3$
$C_3Cr$	3.0	6.5	4.0	HM: $\uparrow=0.4$ $\downarrow=M$
$C_4Cr$	3.0	7.9	4.0	HM: $\uparrow=M$ $\downarrow=2.9$
$C_5Cr$	2.5	9.0	4.0	HM: $\uparrow=0.6$ $\downarrow=M$
$C_6Cr$	3.1	10.3	4.0	HM: $\uparrow=M$ $\downarrow=2.4$
$C_7Cr$	2.5	11.6	4.0	HM: $\uparrow=0.5$ $\downarrow=M$

Whether a periodic  $C_nCr$  linear chain is stable or it can transform to other structures has been examined by an extensive investigation of Born-Oppenheimer surface. Local minima of the total energy have been searched by optimizing the structure starting from transversally displaced chain atoms for varying lattice parameters. The linear chain structure has been found to be stable and energetically favorable relative to zigzag structures.<sup>23</sup>

The phonon calculations of  $C_nCr$ , yielding positive phonon frequencies [ $\Omega_{TO}(k=0) = 89, 92, 411$   $\text{cm}^{-1}$ , and  $\Omega_{LO}(k=0) = 421, 1272, 1680$   $\text{cm}^{-1}$  for  $n=3$ ;  $\Omega_{TO}(k=0) = 13, 71, 353, 492$   $\text{cm}^{-1}$  and  $\Omega_{LO}(k=0) = 489, 1074, 1944, 2102$   $\text{cm}^{-1}$  for  $n=4$ ] corroborate the above analysis of stability. However, for  $n=9$  some of the frequencies become negative, indicating an instability for a large  $n$ . In addition, we performed high temperature ( $T=750$ – $1000$  K) *ab initio* molecular dynamics calculations using Nosé thermostat,<sup>24</sup> where atoms are displaced in random directions. All these tests have provided strong evidence that the linear chain structures with small  $n$  are stable. To weaken the constraints to be imposed by supercell geometry, calculations have been done by using double supercells including two primitive unit cells of the chains. Peierls instability that may cause the splitting of metallic bands at the Fermi level did not occur in  $C_nCr$  linear chain structures. We also examined how an axial strain may affect the half-metallic behavior of these chains. HM character of  $C_4Cr$  was robust under  $\epsilon_z = \pm 0.05$ . The small band gap  $C_5Cr$  remains HM for  $\epsilon_z = 0.05$ , but is rendered a ferromagnetic metal under  $\epsilon_z = -0.05$ . While  $C_3Cr$  changes to a semiconductor under  $\epsilon_z = 0.10$ , it becomes a ferromagnetic metal with  $\mu = 3.1$  under  $\epsilon_z = -0.10$ .

### IV. MAGNETIC AND ELECTRONIC PROPERTIES

In Table I, we summarize the calculated magnetic and electronic properties of  $C_nCr$  ( $1 \leq n \leq 7$ ) linear chains. Spin-polarized electronic band structures are strongly dependent on  $n$ . For example, all the  $C_nCr$  we studied are HM except

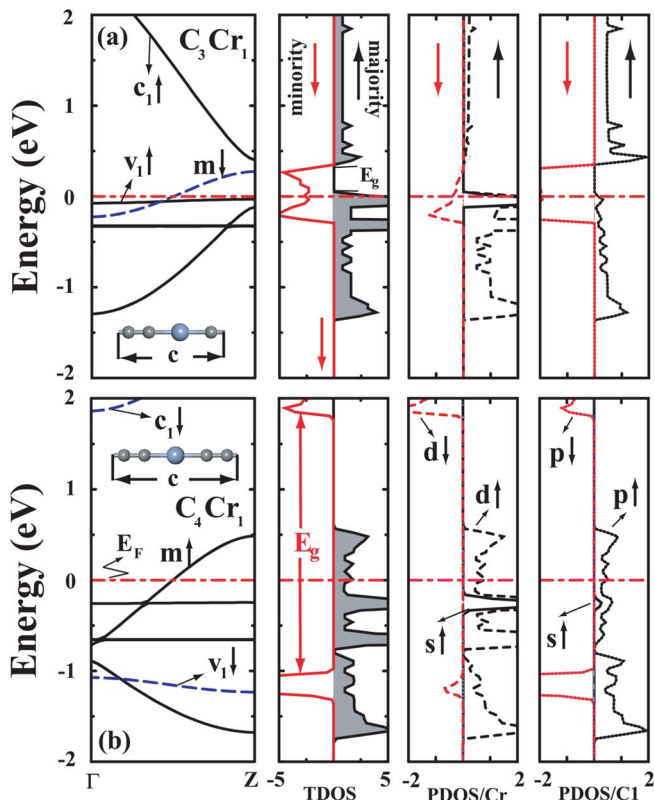


FIG. 2. (Color online) (a) Energy band structure of  $C_3Cr$ ; corresponding TDOS for majority ( $\uparrow$ ) and minority ( $\downarrow$ ) spins; orbital projected local density of states at Cr atom (PDOS/Cr), at C atoms first nearest neighbor to Cr (PDOS/C1). (b)  $C_4Cr$ . State densities with  $s, p, d$  orbital symmetry in PDOS are shown by thin continuous, dotted, broken lines, respectively. Zero of energy is set at  $E_F$ . Metallic band crossing the Fermi level, highest valence and lowest conduction bands are labeled by  $m, v_1$ , and  $c_1$ , respectively.

$CCr$ , which is a semiconductor. For even  $n$ , majority spin bands are metallic, but minority spin bands are semiconducting with large band gaps ( $E_{g,\downarrow} \sim 3$  eV). This situation, however, is reversed for odd  $n$ , where majority spin bands become semiconducting with relatively smaller gaps ( $E_{g,\uparrow} \sim 0.5$  eV), but minority bands are metallic. This even-odd  $n$  disparity is closely related to bonding patterns in different chains. For example, for odd  $n=3$ , respective bond lengths are in  $\text{\AA}$ -C-1.28-C-1.28-C-1.95-Cr-, and for even  $n=4$ , -C-1.25-C-1.33-C-1.25-C-2.1-Cr-. It appears that, while double bonds are forming between all atoms for odd  $n$ , for even  $n$  triple and single bonds form alternately between C atoms, and single bonds occur between C and Cr atoms with relatively longer bond lengths.<sup>14</sup> Consequently, the overlap between Cr and C orbitals and, hence, relative energy positions of bands vary, depending on whether  $n$  is even or odd.

Half-metallic electronic structure and resulting spin-dependent properties of  $C_nCr$  linear chains are shown by the bands and density of states in Fig. 2. The odd-even  $n$  disparity is clearly seen. The double degenerate  $\pi$  band (denoted by  $m\downarrow$  for  $n=3$  or  $m\uparrow$  for  $n=4$ ) is half filled and determines the position of  $E_F$ . The band gap of semiconducting states, which have spin in the direction opposite to that of the  $m$

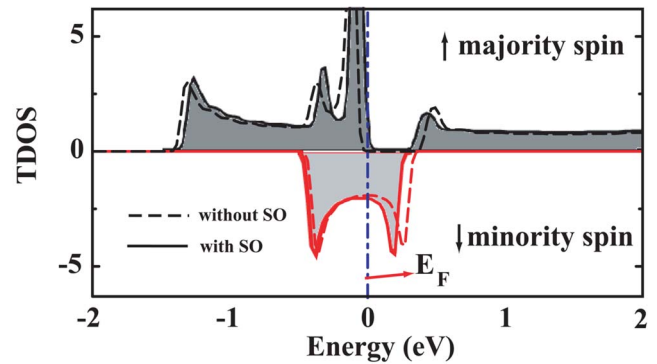


FIG. 3. (Color online) Majority and minority TDOS of  $C_3Cr$  calculated with and without SO coupling.

band, occurs between the filled flat  $v_1$  band and the empty conduction  $c_1$  band. According to these bands, the equilibrium ballistic conductance of the infinite  $C_3Cr$  is  $G_{\downarrow} = 2e^2/h$  for minority spin, but zero for majority spin. The calculated spin projected total density of states (TDOS) in Fig. 2 shows the energy spectrum of majority and minority spin states in an interval  $\pm 2$  eV around  $E_F$ . The band gap for one spin direction and finite density of states at  $E_F$  for the opposite spin are clearly seen. This is a dramatically different finding than those of Refs. 10–13. Orbital projected local densities of states at Cr and C atoms show the orbital composition of the spin-polarized bands. The  $m$  band is composed of Cr-3d and mainly first-neighbor C-2p orbitals at  $E_F$ , that is the  $p-d$  hybridization. The flat  $v_1$  band nearest to  $E_F$  is derived from the Cr-3d and Cr-4s states. The empty  $c_1$  band originates from C-2p and Cr-3d states. Here we note that owing to the negligible overlap between nearest-neighbor Cr-3d orbitals, the formation of flat bands due to Cr-3d orbitals shall cease at large  $n$ , and hence those states become localized.

The effect of spin-orbit (SO) coupling on the HM properties of  $C_3Cr$  has been calculated by using an all-electron DFT (WIEN2K) code.<sup>25</sup> We found the splitting is very small and  $E_T(\text{with SO}) - E_T(\text{without SO}) = -7.9$  meV. As illustrated in Fig. 3, the difference between TDOSs calculated with and without SO coupling is negligible and, hence, the effect is not strong enough to destroy the half-metallic properties. This conclusion obtained for  $C_3Cr$  can apply to other chain structures in Table I, since the Cr—C interaction decays quickly beyond the first nearest neighbors of the Cr atom.

Further insight about the electronic structure and the character of bonding can be gained by examining the charge distributions associated with the selected bands shown in Fig. 4. The charge density of the metallic spin state at  $E_F$  is obtained by averaging charges of states of the  $m$  band having energy  $\pm 0.02$  eV around  $E_F$ . They are formed from the bonding combination (or  $p-d$  hybridization) of C-2 $p_{x,y}$  and Cr-3 $d_{xz,yz}$  valence orbitals of  $C_3Cr$ . In the case of even  $n$  ( $n=4$ ) it corresponds to an antibonding combination of the above orbitals with enhanced Cr-3d contribution. The charge density of the  $v_1$  band is due to nonbonding Cr-4s-3 $d_{z^2}$  orbitals in  $C_3Cr$ . For an even  $n$  case, the C-2 $p_{x,y}$  contribution is pronounced. Charge density of the  $c_1$  band suggests the antibonding combination of  $p-d$  hybridized states.

The band structure and charge density plots suggest that the  $p-d$  hybridization between neighboring C and Cr orbitals

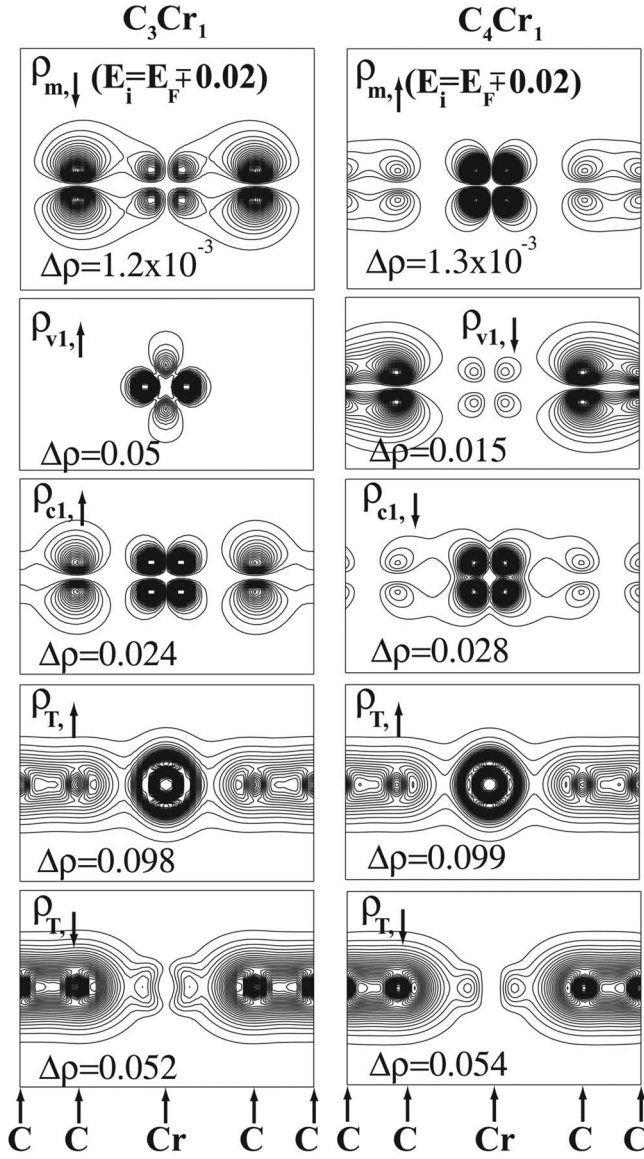


FIG. 4. Charge density contour plots of linear chains of  $C_3Cr$  and  $C_4Cr$  compounds on a plane through the chain axis.  $\rho_{m,\uparrow|\downarrow}$  is the charge density of metallic spin states within energy range  $E_F \pm 0.02$  eV.  $\rho_{v_1,\uparrow|\downarrow}$  and  $\rho_{c_1,\uparrow|\downarrow}$  are the charge density of the highest valence  $v_1$  and the lowest (empty) conduction band  $c_1$ , respectively.  $\rho_{T,\uparrow}$  and  $\rho_{T,\downarrow}$  are total charge density due to majority spin states and minority spin states, respectively.  $\Delta\rho$  is contour spacing.

and resulting exchange splitting of bands in different spin directions give rise to the ferromagnetic ground state of the above chains. An additional ingredient, namely cylindrical symmetry of the  $\pi$  bonds in the carbon chain provides conditions to result in an integer number of excess spin in the unit cell, which is required to achieve half-metallic behavior. The ferromagnetic ground state with  $\mu$  values integer multiple of  $\mu_B$  per unit cell can be understood from a local point of view based on the first Hund's rule. We take  $C_3Cr$  as an example. In Fig. 2(a), three spin-up (one nondegenerate  $v_1$ , one doubly degenerate) bands below  $E_F$  are derived mainly from Cr-3d orbitals. Five of the six electrons on Cr (in these corresponding bands) occupy the majority spin states to yield

$N_{\uparrow}=5$ . The sixth electron occupies the  $p$ - $d$  hybridized, doubly degenerate but only half-filled  $m_{\downarrow}$  band yielding  $N_{\downarrow}=1$ . Consequently,  $N=N_{\uparrow}-N_{\downarrow}=4$ , and hence  $\mu=4 \mu_B$ .

Having discussed the electronic and magnetic properties of  $C_nCr$  linear chains, we briefly discuss the electronic structure of similar compounds of other transition-metal elements. These are  $C_nTi$ ,  $C_nMn$ , and  $C_nFe$ . Among  $C_nTi$  linear chains,  $C_2Ti$  has been found to show half-metallic properties with  $\mu=2.0 \mu_B$ .  $CTi$  and  $C_3Ti$  alloys are semiconductor with  $\mu=0$ , but  $C_5Ti$  is a metal with  $\mu=1.4 \mu_B$ . The  $CMn$  linear chain is a metal with  $\mu=3.0 \mu_B$ , but the other compounds with  $n>1$  are ferromagnetic semiconductors. In the group of  $C_nFe$ , the compounds with even  $n$  are half metals and the others exhibit metallic properties. Interestingly,  $Si_nCr$ ,  $Al_3Ti$ , and  $Al_4Cr$  compounds are half metallic, if they can be held in the linear geometry. However, these compounds are unstable in the linear chain geometry and hence they transform to other energetically more favorable, nonlinear (zigzag) geometries where half-metallic properties are usually destroyed.

## V. CONCLUSION

The present study shows that linear chains of  $C_n(TM)$  compounds ( $TM=Cr, Ti, Mn, Fe$ ) with specific  $n$  can show half-metallic behavior with a diversity of spin-dependent electronic properties. Here, the type and number of atoms in the compound, as well as even-odd  $n$  disparity are critical variables available to engineer nanostructures with spin-dependent properties. The electronic transport properties and the value of  $\mu$  can be modified also by applied axial strain. Not only the periodic structures, but also nonperiodic combinations comprising HM-HM or HM-S (or M) quantum structures and superlattices can be envisaged to obtain desired device characteristics, such as spin-valve effect and spin-resonant tunneling. Since linear carbon chains have been obtained also at the center of multiwall carbon nanotubes,<sup>20</sup>  $C_nCr$  chains can, in principle, be produced inside a nanotube to protect the spintronic device from the undesired external effects or oxidation. In fact, we showed that a strained  $C_7Cr$  compound chain placed inside a (8,0) SWNT can be a HM. Of course, the properties revealed in this study correspond to idealized infinite chain structures and are subject to modifications when the chain size becomes finite. However, for finite but long chains (for example a coil of  $C_nTM$  around an insulating SWNT), the level spacings are still small to gain a bandlike behavior. Also, localization of electronic states due to imperfections in 1D may not lead to serious difficulties when the localization length  $\xi$  is larger than the length of the device. It is also noted that the properties of chains may depend on the type of electrodes and the detailed atomic structure of the electrodes.

In conclusion, we showed that half-metallic properties can be realized in linear chains of carbon-transition-metal compounds presenting a number of exciting properties that can be of fundamental and technological interest for new generation devices. We believe that in view of recent progress made in synthesizing C atomic chains, the present study will bring a different perspective into spintronics.

\*Corresponding author.

Electronic address: ciraci@fen.bilkent.edu.tr

- <sup>1</sup>G. A. Prinz, *Science* **282**, 1660 (1998).
- <sup>2</sup>P. Ball, *Nature (London)* **404**, 918 (2000).
- <sup>3</sup>S. A. Wolf, D. D. Awschalom, R. A. Buhrman, J. M. Daughton, S. von Molnár, M. L. Roukes, A. Y. Chtchelkanova, and T. M. Treger, *Science* **294**, 1488 (2001).
- <sup>4</sup>R. A. de Groot, F. M. Mueller, P. G. van Engen, and K. H. J. Buschow, *Phys. Rev. Lett.* **50**, 2024 (1983).
- <sup>5</sup>W. E. Pickett and J. S. Moodera, *Phys. Today* **54**, 39 (2001).
- <sup>6</sup>J.-H. Park, E. Vescovo, H.-J. Kim, C. Kwon, R. Ramesh, and T. Venkatesan, *Nature (London)* **392**, 794 (1998).
- <sup>7</sup>H. Akinaga, T. Manago, and M. Shirai, *Jpn. J. Appl. Phys., Part 2* **39**, L1118 (2000).
- <sup>8</sup>J. E. Pask, L. H. Yang, C. Y. Fong, W. E. Pickett, and S. Dag, *Phys. Rev. B* **67**, 224420 (2003).
- <sup>9</sup>W.-H. Xie, Y.-Q. Zu, B.-G. Liu, and D. G. Pettifor, *Phys. Rev. Lett.* **91**, 037204 (2003).
- <sup>10</sup>E. Durgun, S. Dag, V. M. K. Bagci, O. Gülseren, T. Yildirim, and S. Ciraci, *Phys. Rev. B* **67**, 201401(R) (2003); E. Durgun, S. Dag, S. Ciraci, and O. Gülseren, *J. Phys. Chem. B* **108**(2), 575 (2004).
- <sup>11</sup>S. Dag, E. Durgun, and S. Ciraci, *Phys. Rev. B* **69**, 121407(R) (2004).
- <sup>12</sup>C. K. Yang, J. Zhao, and J. P. Lu, *Phys. Rev. Lett.* **90**, 257203 (2003).
- <sup>13</sup>V. Rodrigues, J. Bettini, P. C. Silva, and D. Ugarte, *Phys. Rev. Lett.* **91**, 096801 (2003).
- <sup>14</sup>R. Pati, M. Mailman, L. Senapati, P. M. Ajayan, S. D. Mahanti, and S. K. Nayak, *Phys. Rev. B* **68**, 014412 (2003).
- <sup>15</sup>W. Kohn and L. J. Sham, *Phys. Rev.* **140**, A1133 (1965); P. Hohenberg and W. Kohn, *Phys. Rev.* **136**, B864 (1964).
- <sup>16</sup>J. P. Perdew, J. A. Chevary, S. H. Vosko, K. A. Jackson, M. R. Pederson, D. J. Singh, and C. Fiolhais, *Phys. Rev. B* **46**, 6671 (1992).
- <sup>17</sup>Numerical calculations have been performed by using VASP package; G. Kresse and J. Hafner, *Phys. Rev. B* **47**, R558 (1993); G. Kresse and J. Furthmüller, *ibid.* **54**, 11169 (1996). Stability of optimized structures have been confirmed by independent analysis using the software package CASTEP.
- <sup>18</sup>H. J. Monkhorst and J. D. Pack, *Phys. Rev. B* **13**, 5188 (1976).
- <sup>19</sup>Spin-relaxed structure optimization calculations starting with an initial net spin  $S_T=0$  have converged to the values  $S_T = \sum_{n,k}^{occ} (S_{n,k,\uparrow} + S_{n,k,\downarrow}) > 0$ . This situation excludes the possibility of an antiferromagnetic ground state.
- <sup>20</sup>G. Roth and H. Fischer, *Organometallics* **15**, 5766 (1996); X. Zhao, Y. Ando, Y. Liu, M. Jinno, and T. Suzuki, *Phys. Rev. Lett.* **90**, 187401 (2003).
- <sup>21</sup>Nearest-neighbor atoms of the carbon linear chain (C-LC) are bound by the  $\sigma$  bond corresponding to the  $\sigma$  band derived from C-2s and C-2p<sub>z</sub> orbitals along the chain axis and the  $\pi$  bond corresponding to the  $\pi$  band derived from C-2p<sub>x</sub> and C-2p<sub>y</sub> orbitals. The  $\pi$  band is doubly degenerate because of cylindrical symmetry of the linear chain and is half filled. C-LC structure is a metal in ideal conditions and has high cohesive energy of 8.6 eV/atom (that is close to the calculated GGA cohesive energy in diamond structure, 9.5 eV/atom). It is flexible but stiff axially with  $d^2E/d\epsilon_c^2 \sim 119$  eV). Among a large number of 1D chain structures of carbon including planar zigzag and dumbbell structures, C-LC is found to be the only stable structure. Upon relaxation, all other structures are transformed to C-LC with a bond length of 1.27 Å. For other features and transport properties, see for example, S. Tongay, R. T. Senger, S. Dag, and S. Ciraci, *Phys. Rev. Lett.* **93**, 136404 (2004).
- <sup>22</sup>C<sub>5</sub>+Cr initial state is a bound state with  $\mu=5.1$  Bohr magneton and high-spin polarization. We estimate the breaking strain of the linear C<sub>5</sub>Cr HM at the axial strain of  $\epsilon \sim 0.1$  near  $E_T(c) \sim 0$  in Fig. 1(a).
- <sup>23</sup>A slightly zigzag chain structure of C<sub>4</sub>Cr corresponding to a local minimum with a total energy higher than that of the linear chain structure continues to be HM.
- <sup>24</sup>S. Nosé, *Mol. Phys.* **52**, 255–268 (1984).
- <sup>25</sup>This is most accurate calculation using WIEN2K software package with augmented plane waves plus local orbitals and muffin-tin spheres.